Available online at www.sciencedirect.com
SCIENCE DIRECT®
Journal of Nuclear Materials 329–333 (2004) 607–611
journal of nuclear materials
www.elsevier.com/locate/jnucmat

Embrittlement of ER309L stainless steel clad by σ-phase and neutron irradiation

I.S. Kim [a,*], J.S. Lee [a], A. Kimura [b]

[a] Department of Nuclear and Quantum Engineering, Korea Advanced Institute of Science and Technology, 373-1 Guseong-Dong, Yuseong-Gu, Daejeon 305-701, Republic of Korea
[b] Institute of Advanced Energy, Kyoto University, Gokasho, Uji, Kyoto 611-0011, Japan

Abstract

The degradation of mechanical properties in RPV clad by the presence of σ-phase and neutron irradiation was investigated using small punch (SP) tests. The irradiation doses at 290 °C ranged from 5.01×10^{18} to 5.79×10^{19} n/cm^2 (>1 MeV). After irradiation, the increase in SP ductile-to-brittle transition temperature (SP-ΔDBTT) was ≈14 K, independent of the fluence. However, it was more strongly affected by the amount of brittle σ-phase. The cracking appearances in the SP specimens gradually changed from circumferential to radial cracking as a function of test temperature, content of σ-phase and neutron irradiation. These results are discussed in terms of the different fracture stress of each phase as well as the irradiation-induced hardening combined with the changes of governing stress components for crack initiation during deformation by means of finite element stress analysis.

1. Introduction

Welding and joining of blanket structural materials is considered to be a key R&D area for fusion blanket engineering. As a fission–fusion interactive technology, the cladding technology of nuclear reactor pressure vessel (RPV) has been studied to apply it to fusion blanket R&D.

The 300 grade austenitic stainless steels have been used as nuclear reactor pressure vessel (RPV) clad materials for the prevention of corrosion attack in the water coolant system. During solidification of overlay welding, primary δ-ferrite is formed first and then the γ austenite phase is obtained by the transformation reaction of δ-ferrite to γ-phase. However, δ-ferrite remains in the clad because of non-equilibrium rapid solidification. In addition, it is well known that there is a transformation from δ-ferrite to brittle σ-phase after extended exposure to the temperature range of 873–1173 K [1,2]. The presence of σ-phase in an austenitic stainless steel can result in the dramatic loss of ductility and toughness. A study on the influence of σ-phase in a type 310 stainless steel showed that reduction in toughness was about 85% by aging at 973 K for 2 h [2].

At the same time, the mechanical properties of the clad are influenced by in-service exposure to the high energy neutron irradiation at the reactor operating temperature. A few irradiation studies a nuclear RPV clad materials have been carried out and showed a reduction in fracture toughness and an increase in the ductile to brittle transition temperature (DBTT) accompanied by irradiation-induced hardening [3]. Therefore, it is important to understand the embrittlement of RPV clad by σ-phase and neutron irradiation for safe and extended service life operation.

The objectives of this research are to investigate the effect of σ-phase and neutron irradiation on the mechanical properties of RPV clad using the small punch (SP) test. Stress analysis on deformed SP specimens was also carried out to evaluate the cracking criteria of the SP specimens by means of finite element method (FEM).

* Corresponding author. Tel.: +82-42 869 3815; fax: +82-42 869 3810.
E-mail address: iskim@kaist.ac.kr (I.S. Kim).

0022-3115/$ - see front matter © 2004 Elsevier B.V. All rights reserved.
doi:10.1016/j.jnucmat.2004.04.104

2. Experimental

2.1. Material preparations and SP tests

The material used is a type 309L stainless steel weld metal and its chemical compositions are listed in Table 1. Three kinds of RPV clads were produced with submerged arc welding on SA508 cl.3 plates by varying heat input rates from 164.4 (K001 clad) to 188.5 kJ/cm (K002J clad). The claded plates were then post-weld heat treated (PWHT) at 893–901 K for 41 h. Microstructural features of the clads were reported in [5]. The volumetric phase fraction of σ-phase ranged from 1.9 (K001 clad) to 7.9 vol.% (K002J clad). The phase fractions of each clad are shown in Table 1.

Transmission electron microscopy (TEM) disk ($3\phi \times 0.28^{t}$ mm) and coupon ($10\times10\times0.5$ mm^3)-type small punch (SP) specimens were sampled from 2 mm away from the weld fusion line. SP tests were performed at a cross-head speed of 0.2 and 0.4 mm/min for TEM and coupon type specimen, respectively, at temperatures from ~77 to 293 K. Steel balls of 1 and 2.4 mm diameter of which the hardness was over HRC 60 were employed to apply a load to disk and coupon type specimen, respectively. Specific SP energy was evaluated as the area under the load–deflection curve per unit thickness of the given specimen, and the SP ductile-to-brittle transition temperature (SP-DBTT) was defined to be the temperature where the specific SP energy was the average of the maximum SP energy and the lower shelf energy. SEM was used to observe the cracking appearance of the specimens.

2.2. Neutron irradiation

Disk type SP specimens were neutron irradiated in Japan Materials Testing Reactor (JMTR) at 563 ± 1 K up to fluences of 5.1×10^{18} and 1.02×10^{19} n/cm^2 (>1 MeV). Coupon type SP specimens were irradiated at the same temperature up to the fluence of 5.79×10^{19} n/cm^2(>1 MeV) by utilizing the Hi-Flux Advanced Neutron Application Reactor (HANARO) in Korea.

2.3. Finite element analysis

The ABAQUS 6.3 standard finite element analysis (FEA) software was used to simulate the SP test results. Fig. 1(a) presents a brief sketch of the system. The specimen geometry was 0.28 mm in thickness and 3 mm in diameter. The diameter of the ball and the central hole of lower die was 1.0 and 1.6 mm, respectively. Detailed information about the simulation system was reported in [4].

The stress–strain partitioning between δ-ferrite and γ-phase was also simulated by FEA in which a simple cubic bi-crystal was assumed as the configuration geometry, and is shown in Fig. 2(b). The elastic moduli of δ-ferrite and γ-phase were assumed to be 200 and 190 GPa, and Poisson's ratio was 0.3 and 0.28, respectively. True stress versus true strain data of each phase before and after irradiation were extracted from the uniaxial tensile test results by means of the general law of mixtures; $\sigma = \sigma_\delta V_\delta + \sigma_\gamma V_\gamma$, where V_δ, V_γ are the volume fractions, and $\sigma_\delta, \sigma_\gamma$ are the flow stresses for the δ-ferrite and γ-phase, respectively. The flow stress is estimated from the microhardness data [5] with use of an empirical relationship. Uniform displacement was imposed on the both sides of surface (in the X-direction) in a static mode.

3. Results

3.1. SP load–deflection curves

The experimental and simulation results of SP load–deflection curves as a function of test temperature are shown in Fig. 2. In K001 clad, the maximum SP load continuously increased until the test temperature reached at 183 K and the fracture of the specimen occurred in the plastic instability region. Below 183 K, the

Table 1
Chemical compositions of AWS Class ER309L weld metal (w/o) and volumetric phase fractions of each RPV clad

C	Si	Mn	P	S	Cr	Ni	Mo	Co	V	Ti	Cu	Nb	N
0.011	0.36	1.60	0.013	0.001	23.77	13.19	0.06	0.026	0.052	0.09	0.039	0.01	0.045

Index	γ-phase (vol.%)	δ-ferrite (FN[a]) (before PWHT)	δ-ferrite (FN) (after PWHT)	σ-phase (vol.%)
K001	~90	9.1	6.6	1.9
K002		10.4	6.0	3.7
K002J		10.2	2.5	7.9

[a] FN: ferrite number was measured by Ferrite Content Meter, which almost equals to the volumetric percentage.

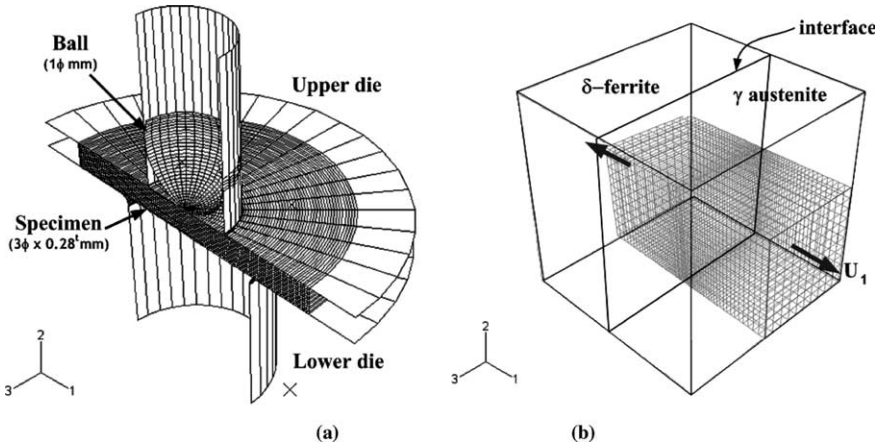

Fig. 1. Schematic diagram of finite elements used in this simulation study for (a) SP loading system and (b) bi-crystal configuration under uniform displacement in the X-direction (U_1).

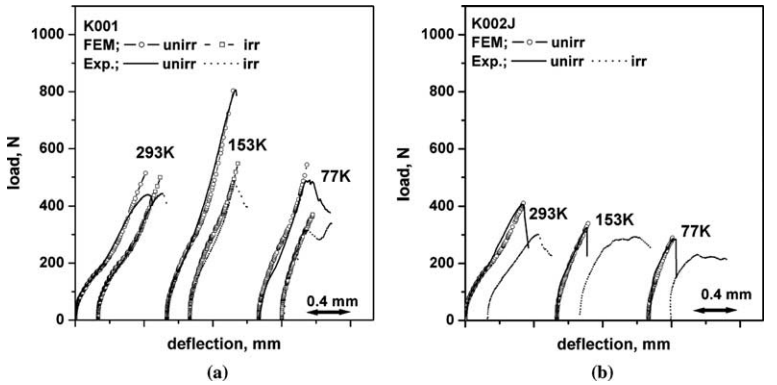

Fig. 2. Experimental and simulation results of TEM disk SP load–deflection curves as a function of test temperature and neutron irradiation, (a) K001 and (b) K002J clad, fluence = 1.02×10^{19} n/cm^2 (>1 MeV).

maximum SP load suddenly decreased and the specimen fractured before reaching the plastic instability region. Similar behavior was observed in a set of load–deflection curves of K002 clad, except that the transition temperature where the maximum SP load started to decrease moved to 223 K. However, the maximum SP load of K002J clad was very small at all test temperatures, resulting that the load was almost same and did not show any transition behavior.

The effect of neutron irradiation on the SP load–deflection curves is also shown in Fig. 2. When the specimen was irradiated up to a fluence of 1.02×10^{19} n/cm^2, the transition temperature shifted to around 223 K in K001 clad. Below this temperature, a reduction in maximum SP load was observed, and finally, serration of SP load occurred at 77 K during deformation. Meanwhile, there were no significant changes of load–deflection curves in K002J clad, showing very small SP load and serration like behavior at all test temperatures except for 293 K. These trends were also identified in the other specimens irradiated up to different fluences.

The finite element simulation results of SP load–deflection curves for the 309L stainless steel in the temperature range from 293 to 77 K give an accurate description of experimental load–deflection curves before and after irradiation.

3.2. SP-DBTT and cracking appearance

The effects of σ-phase and neutron irradiation on the SP energy of the clads are shown in Fig. 3(a). The SP-DBTT was 144 and 165 K in K001 and in K002 clad, respectively. The difference in SP-DBTT between the clads is attributed to the different amount of σ-phase which will play a role of crack initiation site by fracturing at an early stage of deformation. After irradiation, the SP-DBTT moved to higher temperature. However, as shown in Fig. 3(b) the increase in SP-DBTT

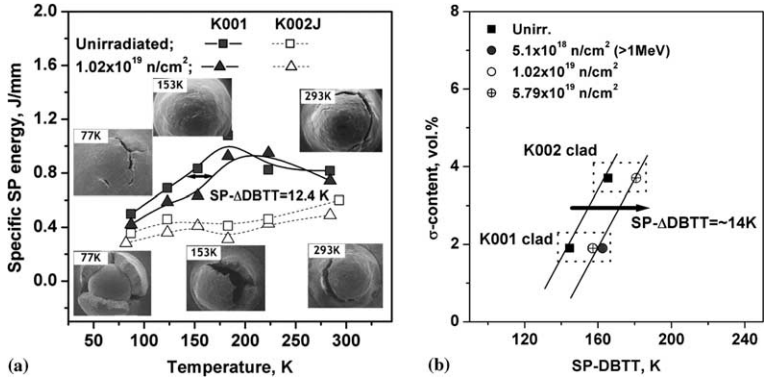

Fig. 3. (a) The variation of SP energy and cracking appearance of RPV clad. Upper and lower three photos in (a) are corresponding to the K001 specimens before and after irradiation, respectively. (b) Effect of σ-phase and neutron irradiation on the SP-DBTT of each RPV clad. The SP-DBTT of K002J clad could not be determined because of significant embrittlement at all test temperatures.

(SP-ΔDBTT) is almost saturated irrespective of the neutron fluence such that the SP-ΔDBTT is ≈14 K.

The cracking appearance of the SP specimens changed from circumferential to radial cracking as a function of test temperature, content of σ-phase and neutron irradiation. As shown in Fig. 3(a), in the unirradiated K001 clad it was completely circumferential at room temperature, and they showed a mixed mode of circumferential and radial cracking below the transition temperature region. Similar results were also observed in K002 specimens except that the dominant cracking was radial at 77 K. On the other hand, the cracking appearance of K002J specimens was completely radial except for tested at room temperature. After irradiation, as shown in Fig. 3(a), although the same transition behavior of cracking appearance was observed in K001 clad, the radial cracking was dominant as the test temperature became low, and complete radial cracking was observed at 77 K. The transition temperature where the cracking appearance changed from circumferential to radial also shifted to higher temperature in K002 clad, while complete radial cracking was shown in K002J clad at all test temperatures.

4. Discussion

4.1. Effect of σ-phase

It was reported that the presence of σ-phase in an austenitic stainless steel resulted in the dramatic loss of ductility and toughness since the σ-phase tended to fracture rather than plastically deformed during deformation [2]. The susceptibility to cracking might coincide with the amount of σ-phase in the clad, and the content of σ-phase in K001, K002 and K002J was 1.9, 3.7 and 7.9 vol.%, respectively. Hence, the severity of embrittlement will increase in the order of K001, K002 and K002J clad, resulting in the shift of SP-DBTT to higher temperature.

As for the SP test, the peak effective stress (σ_{eff}) applied on the specimen bottom surface is developed at the center regions of the specimen at initial deformation of elastic/plastic bending process and transferred to clamped edge with continued deformation. At the initial deformation process, the circumferential stress component is the governing stress state for comprising the effective stress and it is gradually changed by radial stress with progressing deformation [4]. In this situation, cracking of σ-phase will be initiated when the peak effective stress was equal to the fracture stress of σ-phase, 750 MPa [2]. This requirement can be suited at a small amount of deflection in the 309L clad, ≈0.26 and 0.03 mm at 293 and 77 K, respectively. This suggests that the radial cracking becomes dominant because of higher circumferential stress at the initial deformation process. Therefore, in case of K002J clad, since it contained a larger fraction of σ-phase, a significant radial cracking of σ-phase at the entire test temperature regions was inevitable, and then resulted in the lower SP energy.

4.2. Effect of irradiation hardening

The increase in SP-DBTT with irradiation was obviously induced by irradiation hardening combined with the preferential failure of δ-ferrite at low temperatures. The fracture stress of typical ferritic phase is known as ≈1000 MPa when the yield and the tensile strength were 340 and 600 MPa, respectively [6]. High susceptibility of δ-ferrite to embrittlement was clearly shown in Fig. 4(a) through a simulation study of stress (strain) distribution between the δ-ferrite and γ austenite phase. The peak stress to reach the fracture stress of the ferritic phase was developed at the interface of δ/γ-phase and decreased at away from the interface, while the lower strain (ε_{eq}) was available in the δ-ferrite phase. After irradiation, as the

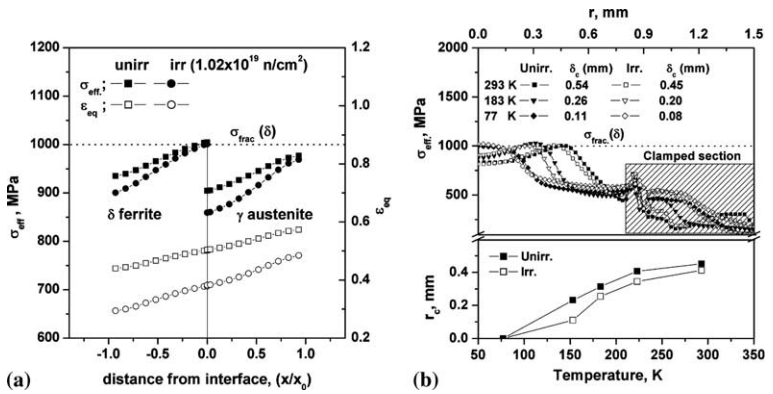

Fig. 4. (a) Stress–strain partitioning at the interface of δ/γ-phase before and after irradiation at 293 K, and (b) variation of critical deflection (δ_c) and critical radial distance (r_c) to reach the ferritic phase fracture stress as a function of test temperature and neutron irradiation.

δ-ferrite phase showed 1.5 times higher hardening than the γ austenite matrix [5], a lower strain was required to attain the fracture stress of ferritic phase, and also the stress intensity at the interface increased.

As shown in Fig. 4(b), to reach the fracture stress of ferritic phase, the K001 SP specimen should be deflected about 0.54, 0.26 and 0.11 mm at 293, 183 and 77 K, respectively, and corresponding critical radial distance (r_c) where the peak stress was developed up to 1000 MPa was 0.45, 0.31 and 0 mm. After irradiation, the deflection and the critical radial distance reduced to 0.45, 0.20, 0.08 mm and 0.41, 0.25, 0 mm at 293, 183 and 77 K, respectively. As pointed out in the previous section, as the critical deflection (δ_c) and critical radial distance (r_c) was reduced by neutron irradiation, the circumferential stress gradually played leading roles for crack initiation by fracturing of δ-ferrite and/or phase separation between the δ-ferrite and γ-phase. Consequently cracking appearance was changed from circumferential to radial cracking, resulting in the shift of SP-DBTT. However, since the σ-phase is the most brittle phase in the clad, the embrittlement is more strongly affected by the content of σ-phase rather than the irradiation induced hardening at present neutron irradiation conditions.

5. Summary

The embrittlement phenomena of RPV clad by σ-phase and neutron irradiation were investigated by SP test. After irradiation, the increase in SP ductile-to-brittle transition temperature (SP-ΔDBTT) was ≈14 K independent of the fluence. However, it was much strongly affected by the amount of brittle σ-phase rather than by the irradiation. When the content of σ-phase was about 7.9 vol.%, the ductile-to-brittle-transition behavior almost disappeared. The cracking appearances in the SP specimens gradually changed from circumferential to radial cracking as a function of test temperature, content of σ-phase and neutron irradiation. The finite element analysis to simulate the stress states of deformed SP specimen well-interpreted the cracking appearance of the specimen before and after irradiation.

References

[1] C.C. Tseng, Y. Shen, S.W. Thompson, M.C. Mataya, G. Krauss, Metall. Mater. Trans. A 25A (1994) 1147.
[2] A.V. Kington, F.W. Noble, Mater. Sci. Eng. A 138 (1991) 259.
[3] F.M. Haggag, W.R. Corwin, R.K. Nanstard, Nucl. Eng. Des. 124 (1990) 129.
[4] J.S. Lee, I.S. Kim, A. Kimura, J. Nucl. Sci. Technol. 40 (9) (2003) 664.
[5] J.S. Lee, I.S. Kim, R. Kasada, A. Kimura, J. Nucl. Mater. 326 (2004) 38.
[6] G.E. Dieter, Mechanical Metallergy, 2nd Ed., McGraw-Hill, New York, 1976, p. 367.